

## RESEARCH ARTICLE

# Functional assessment of the diaphragm by speckle tracking ultrasound during inspiratory loading

Eline Oppersma,<sup>1,2\*</sup> Nima Hatam,<sup>3\*</sup> Jonne Doorduyn,<sup>1,4</sup> Johannes G. van der Hoeven,<sup>1</sup> Gernot Marx,<sup>5</sup> Andreas Goetzenich,<sup>3</sup> Sebastian Fritsch,<sup>5</sup> Leo M. A. Heunks,<sup>1,6\*</sup> and Christian S. Bruells<sup>5\*</sup>

<sup>1</sup>Department of Intensive Care Medicine, Radboud University Medical Center, Nijmegen, The Netherlands; <sup>2</sup>MIRA Institute for Biomedical Technology and Technical Medicine, University of Twente, Enschede, The Netherlands; <sup>3</sup>Department of Thoracic and Cardio-Vascular Surgery, University Hospital RWTH Aachen, Aachen, Germany; <sup>4</sup>Department of Neurology, Radboud University Medical Center, Nijmegen, The Netherlands; <sup>5</sup>Department of Intensive Care, University Hospital RWTH Aachen, Aachen, Germany; and <sup>6</sup>Department of Intensive Care Medicine, VU University Medical Center, Amsterdam, The Netherlands

Submitted 1 February 2017; accepted in final form 11 May 2017

**Oppersma E, Hatam N, Doorduyn J, van der Hoeven JG, Marx G, Goetzenich A, Fritsch S, Heunks LM, Bruells CS.** Functional assessment of the diaphragm by speckle tracking ultrasound during inspiratory loading. *J Appl Physiol* 123: 1063–1070, 2017. First published May 18, 2017; doi:10.1152/jappphysiol.00095.2017.—Assessment of diaphragmatic effort is challenging, especially in critically ill patients in the phase of weaning. Fractional thickening during inspiration assessed by ultrasound has been used to estimate diaphragm effort. It is unknown whether more sophisticated ultrasound techniques such as speckle tracking are superior in the quantification of inspiratory effort. This study evaluates the validity of speckle tracking ultrasound to quantify diaphragm contractility. Thirteen healthy volunteers underwent a randomized stepwise threshold loading protocol of 0–50% of the maximal inspiratory pressure. Electric activity of the diaphragm and transdiaphragmatic pressures were recorded. Speckle tracking ultrasound was used to assess strain and strain rate as measures of diaphragm tissue deformation and deformation velocity, respectively. Fractional thickening was assessed by measurement of diaphragm thickness at end-inspiration and end-expiration. Strain and strain rate increased with progressive loading of the diaphragm. Both strain and strain rate were highly correlated to transdiaphragmatic pressure (strain  $r^2 = 0.72$ ; strain rate  $r^2 = 0.80$ ) and diaphragm electric activity (strain  $r^2 = 0.60$ ; strain rate  $r^2 = 0.66$ ). We conclude that speckle tracking ultrasound is superior to conventional ultrasound techniques to estimate diaphragm contractility under inspiratory threshold loading.

**NEW & NOTEWORTHY** Transdiaphragmatic pressure using esophageal and gastric balloons is the gold standard to assess diaphragm effort. However, this technique is invasive and requires expertise, and the interpretation may be complex. We report that speckle tracking ultrasound can be used to detect stepwise increases in diaphragmatic effort. Strain and strain rate were highly correlated with transdiaphragmatic pressure, and therefore, diaphragm electric activity and speckle tracking might serve as reliable tools to quantify diaphragm effort in the future.

\* E. Oppersma, N. Hatam, L. M. A. Heunks, and C. S. Bruells contributed equally to this work.

Address for reprint requests and other correspondence: L. M. A. Heunks, VU University Medical Center, Amsterdam Department of Intensive Care Medicine, Postbox 7057, 1007 MB Amsterdam, The Netherlands (e-mail: L.Heunks@VUmc.nl).

diaphragm; mechanical ventilation; speckle tracking ultrasound; transdiaphragmatic pressure

UNDER PHYSIOLOGICAL CONDITIONS, the pressure developed by the inspiratory muscles is only  $\pm 5\%$  of maximum inspiratory pressure (17). However, under pathological conditions, such as an acute exacerbation of chronic obstructive pulmonary disease or a failed trial of weaning from mechanical ventilation, the load imposed on the respiratory muscles increases considerably (6, 32). Excessive inspiratory muscle loading may result in fatigue or injury of the diaphragm (16, 35, 37). Accordingly, in selected patients, evaluating respiratory muscle effort may be of clinical relevance (15, 22). Today, measurement of transdiaphragmatic pressure ( $P_{di}$ ) using esophageal and gastric balloons is the gold standard to assess effort of the diaphragm. However, this technique is invasive and requires expertise, and interpretation may be complex (1, 15).

Diaphragmatic function has been studied by B-mode and M-mode ultrasound (3, 29, 31). Fractional thickening (FT) of the diaphragm has been used in previous studies to quantify effort of the diaphragm (3, 18, 25). However, Goligher et al. (19) reported low correlations ( $r^2 = 0.28$ ) in healthy subjects between  $P_{di}$  and diaphragmatic thickening fraction, indicating limited validity of FT to quantify diaphragm effort.

Two-dimensional deformation ultrasound or speckle tracking (ST) ultrasound is an innovative ultrasound technique enabling distinct assessment of muscle function (2). The gray value pattern in ultrasound images remains relatively constant for any small region in muscle tissue; this is called a speckle. In the speckle tracking technique, a defined cluster of speckles is tracked from one frame to another during a contractile cycle. This enables the angle-independent, two-dimensional quantification of the percentage of deformation (strain; %) and deformation velocity (strain rate; s). For readers with additional interest in basic deformation imaging methodology, we may humbly refer to the references of Collier et al. (9) and Smiseth et al. (38).

Speckle tracking echocardiography has become a popular tool for both research and clinical purposes (2, 10, 26, 44). Previously, we have demonstrated the feasibility of ST of the diaphragm during respiratory muscle unloading with noninva-

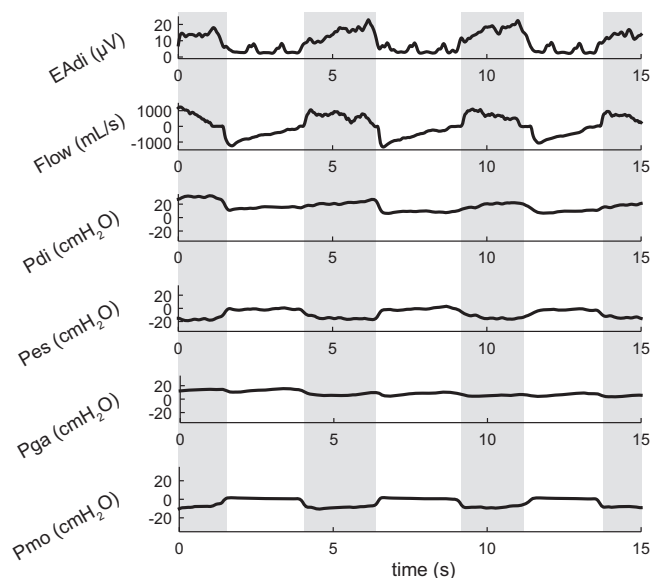


Fig. 1. Representative tracing of electric activity of the diaphragm ( $E_{Adi}$ ), flow, electric activity of the diaphragm ( $P_{di}$ ), esophageal pressure ( $P_{es}$ ), gastric pressure ( $P_{ga}$ ), and mean mouth pressure ( $P_{mo}$ ) during inspiratory threshold loading [20% of maximum inspiratory pressure (MIP); random subject]. Shaded areas are inspiration.

sive ventilation (20). ST has not been validated as a measure of diaphragm contractility using  $P_{di}$  as a gold standard. We hypothesize that strain and strain rate, obtained by ST, can be used to quantify diaphragm contractility during inspiratory loading, and this study aims to investigate the validity of these parameters. Part of this work has been presented previously at the international conference of the European Respiratory Society (33).

## MATERIALS AND METHODS

**Subjects.** We enrolled 15 healthy volunteers with a body mass index of  $<25 \text{ kg/m}^2$ . This study was conducted at the Radboud University Medical Center, and the protocol was approved by the local ethics review committee and conducted in accordance with the Declaration of Helsinki and its later amendments. All subjects gave their written informed consent. Preexisting neuromuscular disorders or lung diseases were defined as exclusion criteria.

**Measurements.** A multielectrode esophageal catheter with two balloons (NeuroVent Research, Toronto, ON, Canada) was inserted, and the balloons were inflated with air, as described previously (13, 14). The flow, electric activity of the diaphragm ( $E_{Adi}$ ), esophageal pressure ( $P_{es}$ ), and gastric pressure ( $P_{ga}$ ) were recorded continuously (13).  $E_{Adi}$  signals were amplified and digitized (Porti 16, 22 bits, 71.5 nV/least significant bit; TMSi) at a sampling frequency of 2 kHz. Pressure signals and flow were digitized (Porti 16, 22 bits, 1.4  $\mu\text{V}$ /least significant bit; TMSi) at a sampling frequency of 2 kHz. Data were stored and buffered on an external drive for offline analysis. Transdiaphragmatic pressure ( $P_{di}$ ) was calculated as  $P_{es}$  subtracted from  $P_{ga}$ . Tidal volume ( $V_T$ ) was obtained by digital integration of the flow signal. Diaphragm ultrasound was performed using a 9-MHz linear transducer with a Vivid E 9TM ultrasound machine (General Electric Healthcare, Horton, Norway).

**Study protocol.** The protocol starts with the measurement of maximum inspiratory pressure (MIP). The mean mouth pressure ( $P_{mo}$ ) during sustained maximum inspiration for 1 s, as recommended by the ATS/ERS statement on respiratory muscle testing (1) against a closed valve at functional residual capacity, is defined as the MIP. The

maneuver is repeated at least five times until three reproducible efforts, with  $<10\%$  variance, are obtained. Subjects were seated in the upright position.

**Inspiratory loading.** An in-house-developed inspiratory threshold apparatus, modified from Chen et al. (7), was used to perform negative pressure threshold loading. In short, the device consisted of a cylindrical adjustable pressure chamber, which was connected to a nonrebreathing valve. The negative pressure was generated by a powerful commercially available vacuum cleaner. Pressure in the chamber was measured continuously using a differential pressure transducer (range  $\pm 375 \text{ mmHg}$ ; Freescale). The dead space of the device can be estimated at  $\sim 600 \text{ ml}$ . Subjects were seated in the upright position with uncast abdomen, breathing through a mouthpiece while wearing a nose clip. Inspiratory loading of 0, 10, 20, 30, 40, and 50% of MIP was applied in random order. Every loading task was applied for 3 min and alternated with 5 min of unloaded breathing. During the loading tasks,  $E_{Adi}$ ,  $P_{es}$ ,  $P_{ga}$ ,  $P_{mo}$ , and flow were recorded continuously (Fig. 1).

**Ultrasound recording.** The ultrasound transducer was positioned in the right anterior axillary line longitudinal to the body axis (between the 9th–11th intercostal space) (Fig. 2 top, and Supplemental Video

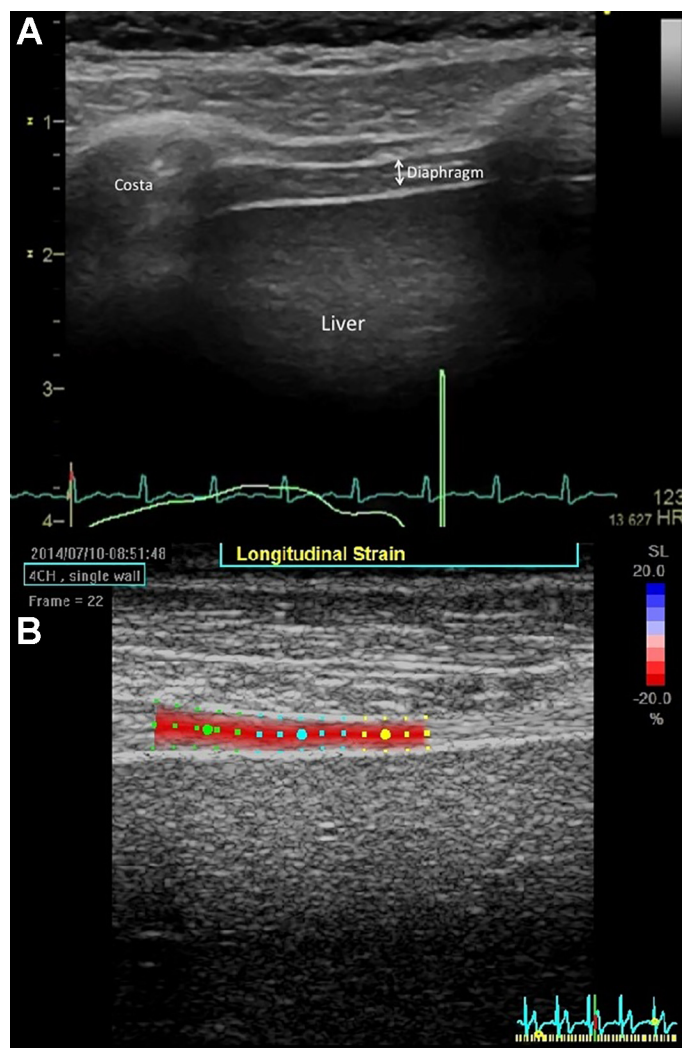


Fig. 2. A: B-mode picture of a scanned diaphragm area between chest wall and liver. Double arrow indicates the diaphragm between to hyperechoic lines, which are the equivalent to the border between diaphragm/pleura and peritoneum. Note the gray “dots” inside the diaphragm (“speckles”). B: region of interest tracked by the software.

S1; Supplemental Material for this article can be found online at the *Journal of Applied Physiology* web site). We chose the strongly longitudinal approach vs. the individual intercostal space to reduce angle dependence of the measurements. The hemidiaphragm is thereby displayed above the liver as a central, less echogenic layer between the peritoneal and pleural echogenic layer (Fig. 2 top, and Supplemental Video S1). The region of interest (ROI) was positioned as described below during the offline data analysis (Fig. 2, bottom). This probe position was marked on the skin for the purpose of standardization (18). Ultrasound recordings of the diaphragm were made at the final minute of every inspiratory loading task. A 10-s recording with the highest possible frame rate was used for offline analysis. Strain describes the relative change in length between an initial reference state ( $L_0$ ) and the compressed/shortened state ( $L$ ). The conventional strain is defined as:  $\epsilon = (L - L_0)/L_0$ . Positive strain means stretching, whereas negative strain means shortening. An increase in strain, as described in the following data presentation, refers to a more negative value of strain, and thus an increase in shortening; e.g.,  $-10$  to  $-15\%$  corresponds to an increase in strain (or shortening).

Strain rate indicates the rate of deformation as follows:  $\epsilon'' = d\epsilon/dt$ . Strain rate is an instantaneous measurement not requiring a relation to a reference state.

Examples for insufficient and sufficient tracking are displayed in Supplemental Videos S1 and S4.

**Data analysis.**  $E_{A_{di}}$ ,  $P_{es}$ ,  $P_{ga}$ ,  $P_{di}$ ,  $P_{mo}$ , and flow were analyzed offline using algorithms developed in Matlab R2013a (The Mathworks, Natick, MA).  $E_{A_{di}}$  refers to a method using a standard electrode, acquisition, and analysis system to overcome signal filtering and processing effects when quantifying the diaphragm, as described previously (13).

$P_{es}$  at end expiration was calculated as a measure of lung volume and corrected for active expiration (36). The recorded ultrasound data were analyzed offline, with the speckle tracking technique using the two-dimensional (2D) strain modality of EchoPac's Q-analysis tool (software version BT 12; General Electric Healthcare). Although the GE software is designed to trigger by the ECG signal by default, the cine loops were adjusted to one entire breathing cycle based upon simultaneously recorded respiratory curves. The software allows for manually moving the loop to the desired cycle, resulting in an adequate measurement independent of the cardiac cycle. The ROI was placed at the lower echogenic line (peritoneal line) to the upper echogenic line (pleural line) starting at the right side of the sector (cranial) and ending at the left sector side (caudal) with approximately five to seven points (Fig. 2 bottom, and Supplemental Videos S2 and S3). In some loops, especially in the higher loading steps (40 and 50% MIP), several attempts of ROI placement were necessary to achieve proper tracking. Here, fewer points with a narrower ROI had to be selected to allow adequate tracking. We refer to Supplemental Videos S4 for an example of not appropriate tracking. In general, these offline measurements can be finished in several minutes.

FT was also calculated from the ultrasound images. In the 2D image, diaphragmatic thickness at end expiration and end inspiration was measured at the same point following the longitudinal downward motion of the respective location. FT was measured at minimum in three different breaths and calculated by the following equation: (thickness at inspiration – thickness at expiration)/thickness at expiration. The quality of the recorded loops varied in some volunteers, depending on the load and general movement of the thorax, especially in high-loading steps. Loops were discarded from the analysis if no sufficient border tracking could be developed (see Supplemental Videos S5 and S6).

**Statistical analysis.** Values are presented as means  $\pm$  SD, and  $P < 0.05$  was considered significant. Statistical analyses were performed with SPSS 21.0 (SPSS, Chicago, IL). Repeated-measures one-way ANOVA was used to test the effect of inspiratory loading on  $E_{A_{di}}$ ,  $P_{es}$  at end expiration,  $P_{di}$ , strain, strain rate, and FT. Correlations between

$E_{A_{di}}$ ,  $P_{di}$ , FT, and strain and strain rate were assessed using repeated-observations correlation (4, 5). This method accounts for multiple measurements within subjects by removing the differences between subjects and looking only at changes within subjects.

## RESULTS

**Subjects.** All included subjects (baseline characteristics: male/female, 7/8; age,  $21.3 \pm 2.3$  yr; BMI  $21.6 \pm 1.7$  kg/m<sup>2</sup>) completed the protocol without adverse effects. Two data sets were lost from analysis due to technical issues (file damage). Mean MIP value for the group was  $100 \pm 32$  cmH<sub>2</sub>O.

**Physiological measurements.** Mean mouth pressure for all subjects was  $-1.2 \pm 0.4$ ,  $-13.7 \pm 4.6$ ,  $-26.3 \pm 7.6$ ,  $-37.9 \pm 11.7$ ,  $-49.9 \pm 14.3$ , and  $-59.7 \pm 16.9$  cmH<sub>2</sub>O for 0–50% inspiratory loading. The stepwise increase in inspiratory loading resulted in an increase in both  $P_{di}$  and  $E_{A_{di}}$  (Fig. 3).  $P_{di}$  increased from  $14.3 \pm 5.9$  cmH<sub>2</sub>O at unloaded breathing via the mouthpiece to  $60.8 \pm 24.4$  cmH<sub>2</sub>O at 50% loading. Likewise,  $E_{A_{di}}$  increased from  $20.3 \pm 11.3$   $\mu$ V at zero loading to  $66 \pm 23.2$   $\mu$ V at 50% loading.  $P_{es}$  at end expiration decreased from  $-3.7 \pm 3.7$  cmH<sub>2</sub>O at zero loading to  $-6.0 \pm 5.3$  cmH<sub>2</sub>O at 50% loading ( $P = 0.03$ ). There were no changes in  $V_T$  or respiratory frequency during the different inspiratory loading steps (Table 1).

**Ultrasound assessment.** In all assessable data sets, a ROI could be tracked in the offline ultrasound analysis during diaphragm contraction and relaxation. Table 2 shows the thickness of the diaphragm at end expiration, end inspiration, and thickening fraction as well as the repeatability coefficients. Repeated-measures one-way ANOVA showed that with increasing load both strain and strain rate increased ( $P < 0.001$ ). Strain increased from  $-22 \pm 7.6\%$  at zero loading to  $-41.5 \pm 10.1$  at 50% loading. Consistent with strain, strain rate increased from  $-0.48 \pm 0.2$  s at zero loading to  $-1.5 \pm 0.7$  s at 50% loading (Fig. 3).

Strain and strain rate were both significantly correlated with  $E_{A_{di}}$  and  $P_{di}$ . Strain vs.  $E_{A_{di}}$  showed a correlation of  $r^2 = 0.60$  ( $P < 0.0001$ ), whereas strain vs.  $P_{di}$  data showed a correlation of  $r^2 = 0.72$  ( $P < 0.0001$ ). Correlations between strain rate and  $P_{di}$  ( $r^2 = 0.80$ ,  $P < 0.0001$ ) and between strain rate and  $E_{A_{di}}$  ( $r^2 = 0.66$ ,  $P < 0.0001$ ) were even higher than those reported for strain (Fig. 4).

Diaphragm thickness during zero loading was  $2.4 \pm 0.7$  and  $3.8 \pm 1.2$  mm during end expiration and end inspiration, respectively, and did not change during inspiratory loading (Table 1). Consequently, FT was not affected by incremental inspiratory loading ( $P = 0.70$ ). Also, no significant correlations between  $E_{A_{di}}$  and FT ( $P = 0.790$ ), between  $P_{di}$  and FT ( $P = 0.495$ ), or between FT and strain ( $P = 0.654$ ) and strain rate ( $P = 0.364$ ) were found.

## DISCUSSION

The present study is the first to evaluate speckle tracking ultrasound of the diaphragm during inspiratory muscle loading. We found that the ST parameters strain and strain rate are highly correlated with  $P_{di}$ , the gold standard for diaphragmatic contractility, and also with  $E_{A_{di}}$ . Strain rate had the highest correlation with  $P_{di}$  and  $E_{A_{di}}$ . Furthermore, ST proved to be superior to diaphragm fractional thickening, as assessed by conventional ultrasound to quantify diaphragmatic effort.

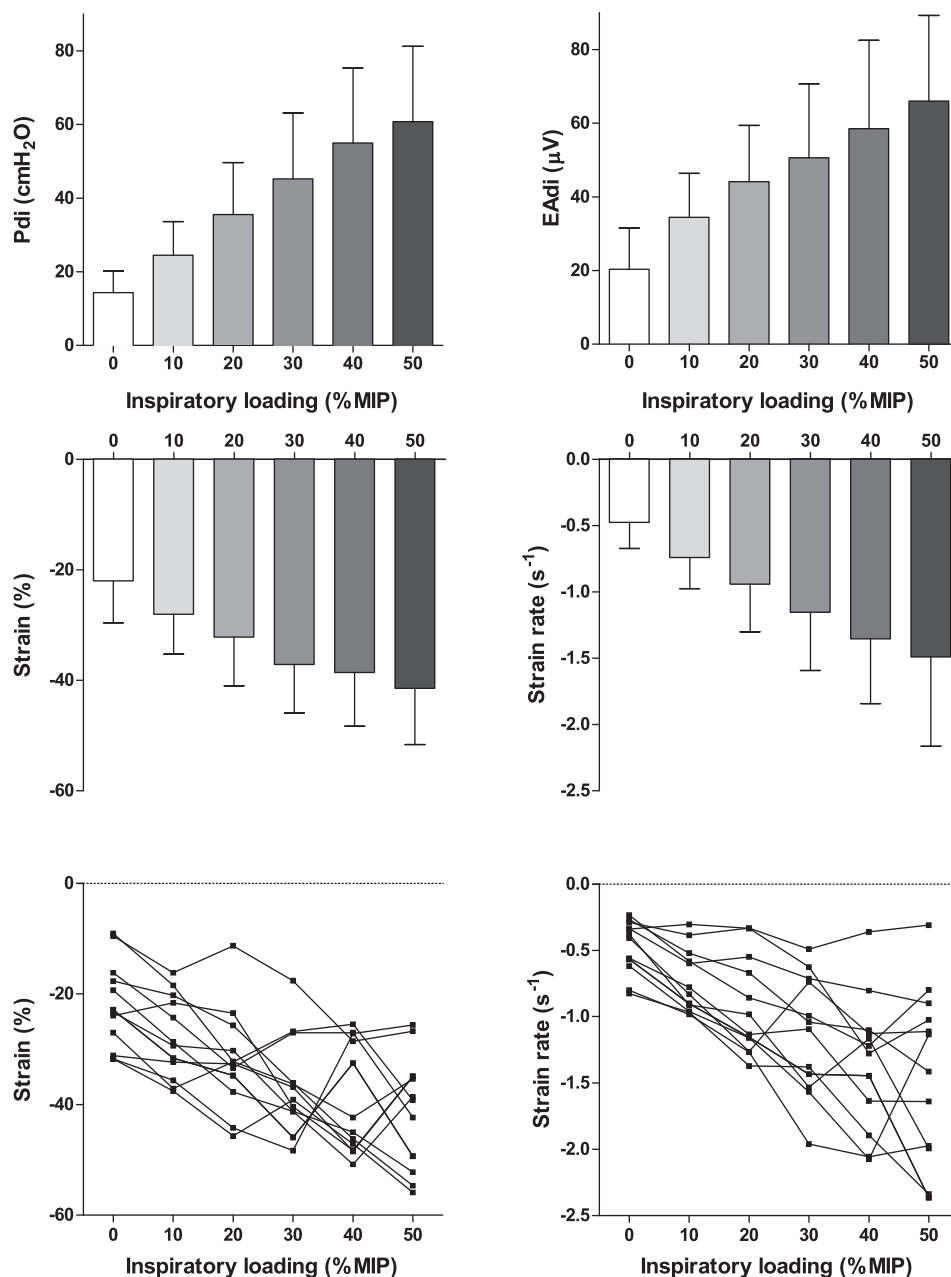


Fig. 3. Top and middle: means ± SD of E<sub>Adi</sub>, P<sub>di</sub>, strain, and strain rate as function of inspiratory loading (%MIP) for all subjects. Repeated measures 1-way ANOVA showed a significant effect of increased loading on all variables (*P* < 0.001). Bottom: individual data of all subjects, strain, and strain rate as function of inspiratory loading (%MIP).

*Validation of the physiological model.* Two methods for loading of the diaphragm have been described in the literature: inspiratory threshold loading and inspiratory resistive loading. The load imposed by the latter method is highly dependent on the inspiratory flow generated by the subject; low flow will

result in minimal loading. We used a threshold load, as this may best reflect loading in intensive care patients where elastic properties of the respiratory system are increased due to pulmonary edema, chest wall edema, and pleural fluid. Our setup for inspiratory threshold loading was modified from Chen et al.

Table 1. Physiological response to the different loading steps

	Inspiratory loading (%MIP)						<i>P</i> Value
	0	10	20	30	40	50	
V <sub>T</sub> , ml	1,076 ± 350	1,183 ± 427	1,147 ± 425	1,053 ± 346	1,049 ± 418	936 ± 329	0.161
Resp. frequency, breaths/min	13.5 ± 4.2	15.3 ± 4.4	15.6 ± 5.4	16.7 ± 6.1	16.1 ± 5.7	17.3 ± 5.7	0.133
Diaphragm thickness end expiration, mm	2.4 ± 0.7	2.4 ± 0.6	2.6 ± 0.5	2.6 ± 0.7	2.5 ± 0.6	2.4 ± 0.7	0.783
Diaphragm thickness end inspiration, mm	3.8 ± 1.2	4.0 ± 1.5	4.1 ± 1.7	3.9 ± 1.8	4.0 ± 1.4	3.6 ± 1.4	0.452

Values are means ± SD. MIP, maximum inspiratory pressure; V<sub>T</sub>, tidal volume. *P* value is given of repeated-measures 1-way ANOVA.

Table 2. Thickness of the diaphragm at end expiration and end inspiration and thickening fraction

	End-Expiration Thickness	End-Inspiration Thickness	Thickening Fraction, %
0%	2.4 ± 0.7	3.8 ± 1.2	59.9 ± 32.1
10%	2.4 ± 0.6	4.0 ± 1.5	67.9 ± 35.0
20%	2.6 ± 0.5	4.1 ± 1.7	55.0 ± 39.2
30%	2.6 ± 0.7	3.9 ± 1.8	48.9 ± 34.7
40%	2.5 ± 0.6	4.0 ± 1.4	61.5 ± 48.1
50%	2.4 ± 0.7	3.6 ± 1.4	50.6 ± 46.7
Repeatability coefficient	1.07 mm	2.54 mm	85.2%

Data are shown as means ± SD in mm for all subjects. Bottom row shows the values for the repeatability coefficient of the measurements.

(7). Figure 1 shows a representative example of one subject at loading of 10% of MIP. It should be noted that at 0% inspiratory loading  $P_{di}$ ,  $E_{A_{di}}$ ,  $V_T$ , and TF were higher than expected for a healthy subject (13). This is most likely the result of the additional resistance and instrumental dead space imposed by the experimental device. As expected, increasing the inspiratory load as a percentage of MIP resulted in an increase in  $P_{di}$  (Fig. 3).

**Speckle tracking ultrasound of the diaphragm.** Tracking of unique grayscale scatter patterns, i.e. “speckles,” is one of the most useful tools in cardiac imaging to assess cardiac function and is closely correlated with contractile myocardial function and outcome (2, 26, 41, 44). These speckle patterns are the ultrasonic correlate of interferences of ultrasound inside the tissue, i.e., different tissue patterns (muscle fibers, epimysium, etc.) and their movement toward each other. Movement of speckle patterns reflects myofibrils/muscle tissue during its contraction, although speckles do not represent specific single myofibrils. It is important to mention that strain and strain rate

approximate contractile function but are not equal to contraction (11, 43).

Software tools to derive deformation data out of two- or three-dimensional ultrasonic cine loops are usually designed to track speckles in between endomyocard and epimyocard as hyperechoic leading structures. The parameters strain and strain rate define different but load-dependent variables; muscle deformation (strain) and deformation velocity (strain rate) can be inferred. Importantly, in contrast to conventional ultrasound techniques, this measure is probe angle independent, which is of fundamental importance if the diaphragm is investigated. An important advantage of ST is that, compared with conventional ultrasound, the ST software recognizes the same region of the diaphragm. A limitation is that defining ROIs and the software calculations are based on an algorithm patented by GE, which is not open to the public.

Within the current study, we did not assess intra- and interobserver variability. This has been evaluated extensively by Orde et al. (34). Their study demonstrated that ST of the right diaphragm is feasible and reproducible (34). Diaphragm images were recorded from the end of expiration through the end of inspiration at 60% maximal inspiratory capacity. The current study is the first to demonstrate that diaphragm strain and strain rate are highly correlated with  $P_{di}$ , the gold standard for diaphragm effort. In addition, a high correlation was found between these two ST measures and  $E_{A_{di}}$ .

**Fractional thickening during inspiratory loading.** Diaphragm FT during inspiration as a measure for loading has been studied previously (12, 19, 40, 42). Umbrello et al. (40) found that diaphragm thickening is a reliable indicator of respiratory effort, and Vivier et al. (42) as well found a parallel decrease in FT and the diaphragmatic pressure-time product per breath during noninvasive ventilation with increasing lev-

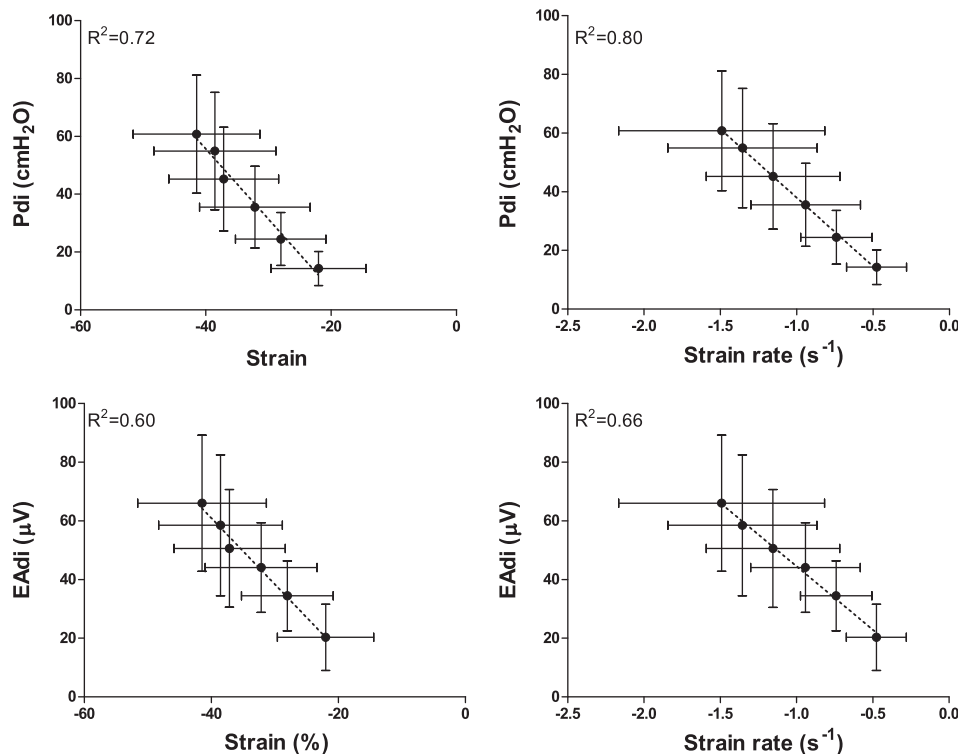


Fig. 4. Correlation of  $P_{di}$  and  $E_{A_{di}}$  vs. strain and strain rate for all subjects during inspiratory loading from 0 to 50%.

els of support. Goligher et al. (19) reported a rather low but significant correlation ( $r^2 = 0.3$ ;  $P < 0.01$ ) for FT vs. both  $P_{di}$  and  $E_{A_{di}}$  in healthy subjects ( $n = 5$ ) (19). In the current study, no significant correlation between FT and  $P_{di}$  or  $E_{A_{di}}$  was found. To evaluate whether insufficient ultrasound training of our investigators contributed to this discrepancy, the repeatability coefficient of thickness at end expiration was calculated, as this measure is unaffected by our loading protocol (Table 2). This demonstrates that the relatively high variation in FT in the present study is due mainly to the variation in thickness at end inspiration but also that the repeatability at end expiration in our study was relatively high compared with the study by Goligher et al. (1.07 vs. 0.2 mm in the current study and the Goligher et al. study, respectively) (19).

Another possible explanation for the apparent discrepancy with the study by Goligher et al. (19) is the difference in inspiratory loading protocol used. In their study, thickness was measured at different lung volumes, whereas in our study inspiratory threshold loading was imposed, whereas volume was kept more or less constant (Table 1), which may have important implications. Finally, the current study is a single point study and not a follow-up study where patients were ventilated; our population consisted of healthy, not ventilated subjects, which also may account for the discrepancy with the study by Goligher et al. (19). In a study by Cohn et al. (8), healthy subjects were instructed to target specific lung volumes up to total lung capacity. A nonlinear relationship was found for FT vs. lung volume (polynomial equation was calculated with an  $r^2$  of 0.99). Because subjects were instructed to keep the glottis open, the diaphragm was active at the targeted lung volumes, and thus changes in diaphragm thickness resulted from changes in volume and pressure. When thickness is measured at different lung volumes with closed glottis (diaphragm relaxed), volume affects diaphragm thickness only at lung volume  $>50\%$  of vital capacity (19). Finally, Ueki et al. (39) measured diaphragm during maximal inspiratory effort against a closed valve (isovolumetric). They reported a strong correlation between maximum inspiratory pressure and diaphragm FT ( $r^2 = 0.67$ ). The relationship between isometric inspiratory pressure and FT was not studied systematically.

Apparently, the relationship between diaphragm thickness and effort ( $P_{di}$ ,  $E_{A_{di}}$ ), is complex and depends upon other possible factors on the pressure developed, lung volume and thoracic cage configuration (8, 19, 39), which may explain the poor or absent correlation between FT and  $P_{di}$  in the studies discussed. However, because chest cage configuration was not controlled in this study, we cannot derive any conclusions about the influence of the chest cage configuration on the relation between diaphragm thickness and effort.

The strong correlation between  $P_{di}$  and strain as well as strain rate in the current study indicates that speckle tracking ultrasound-derived parameters may provide a good estimation of diaphragm effort, at least under inspiratory threshold loading. The performance of speckle tracking ultrasound under different loading conditions (isometric contractions, high inspiratory volume) remains to be evaluated.

*Future perspectives and clinical implications.* Regarding deformation analysis of the diaphragm, the software deriving the ST data has to be adapted to diaphragmatic ultrasonic morphology, allowing quick, easy, and reproducible analysis, preferably on site. The offline setting of the actual data analysis is

currently the only way to ensure proper data analysis, which hampers its use as bedside tool. In echocardiography, most vendors provide a simplified software tool for ST, allowing measurements on site.

Only a few days of controlled mechanical ventilation are associated with atrophy of the diaphragm (23, 30). The reduction in diaphragm force, assessed by bilateral magnetic stimulation of the phrenic nerves, is  $\sim 30\%$  in the first 5–6 days of invasive mechanical ventilation, indicating the rapid development of diaphragm weakness (24). Despite the growing evidence that diaphragm weakness develops in critically ill patients and contributes to weaning failure and thus prolonged ventilation (21, 24, 28), respiratory muscle function is poorly monitored in these patients. Importantly, current state of the art techniques for monitoring, such as  $E_{A_{di}}$  and  $P_{di}$ , are invasive and not widely available, and their interpretation may be rather complex (15). An ideal assessment of diaphragm function must be available at bedside, fast and easy to acquire, and allow standardized quantification. Guiding of ventilator weaning and assessing diaphragm contractile force during spontaneous breathing trials and/or pressure support ventilation might allow us to adapt ventilation and weaning protocols individually. Both sufficient loading and prevention of excessive loading are decisive for weaning success. ST of the diaphragm might serve as a diagnostic tool that can provide direct insight into diaphragm activity and force generation.

In conclusion, speckle tracking ultrasound as noninvasive techniques can be used to detect stepwise increases in diaphragmatic effort. Deformation (strain) and deformation velocity (strain rate) were highly correlated with transdiaphragmatic pressure and electric activity of diaphragm. Speckle tracking ultrasound might serve as reliable tool to guide weaning at the bedside in the future.

## DISCLOSURES

G. Marx reports grants and personal fees from BBraun Melsungen and grants and personal fees from Adrenomed outside of the submitted work; In addition, G. Marx has a patent Modulation of TLR4-signaling pathway pending. All other authors have nothing to disclose.

## AUTHOR CONTRIBUTIONS

E.O., N.H., J.D., L.M.H., and C.S.B. conceived and designed research; E.O., N.H., A.G., L.M.H., and C.S.B. performed experiments; E.O., N.H., J.D., A.G., L.M.H., and C.S.B. analyzed data; E.O., N.H., J.D., A.G., S.F., L.M.H., and C.S.B. interpreted results of experiments; E.O., N.H., J.D., L.M.H., and C.S.B. prepared figures; E.O., N.H., J.D., L.M.H., and C.S.B. drafted manuscript; E.O., N.H., J.D., J.G.v.d.H., G.M., A.G., S.F., L.M.H., and C.S.B. edited and revised manuscript; E.O., N.H., J.D., J.G.v.d.H., G.M., A.G., S.F., L.M.H., and C.S.B. approved final version of manuscript.

## REFERENCES

1. American Thoracic Society/European Respiratory Society. ATS/ERS statement on respiratory muscle testing. *Am J Respir Crit Care Med* 166: 518–624, 2002. doi:10.1164/rccm.166.4.518.
2. Amundsen BH, Helle-Valle T, Edvardsen T, Torp H, Crosby J, Lyseggen E, Støylen A, Ihlen H, Lima JA, Smiseth OA, Slørdahl SA. Noninvasive myocardial strain measurement by speckle tracking echocardiography: validation against sonomicrometry and tagged magnetic resonance imaging. *J Am Coll Cardiol* 47: 789–793, 2006. doi:10.1016/j.jacc.2005.10.040.
3. Ayoub J, Cohendy R, Prioux J, Ahmaidi S, Bourgeois JM, Dauzat M, Ramonatxo M, Préfaut C. Diaphragm movement before and after cholecystectomy: a sonographic study. *Anesth Analg* 92: 755–761, 2001. doi:10.1213/0000539-200103000-00038.

4. Bland JM, Altman DG. Calculating correlation coefficients with repeated observations: Part 1—Correlation within subjects. *BMJ* 310: 446, 1995. doi:10.1136/bmj.310.6977.446.
5. Bland JM, Altman DG. Calculating correlation coefficients with repeated observations: Part 2—Correlation between subjects. *BMJ* 310: 633, 1995. doi:10.1136/bmj.310.6980.633.
6. Carlucci A, Ceriana P, Prinianakis G, Fanfulla F, Colombo R, Nava S. Determinants of weaning success in patients with prolonged mechanical ventilation. *Crit Care* 13: R97, 2009. doi:10.1186/cc7927.
7. Chen RC, Que CL, Yan S. Introduction to a new inspiratory threshold loading device. *Eur Respir J* 12: 208–211, 1998. doi:10.1183/09031936.98.12010208.
8. Cohn D, Benditt JO, Eveloff S, McCool FD. Diaphragm thickening during inspiration. *J Appl Physiol* (1985) 83: 291–296, 1997.
9. Collier P, Phelan D, Klein A. A test in context: myocardial strain measured by speckle-tracking echocardiography. *J Am Coll Cardiol* 69: 1043–1056, 2017. doi:10.1016/j.jacc.2016.12.012.
10. Crosby J, Amundsen BH, Hergum T, Remme EW, Langeland S, Torp H. 3-D speckle tracking for assessment of regional left ventricular function. *Ultrasound Med Biol* 35: 458–471, 2009. doi:10.1016/j.ultrasmedbio.2008.09.011.
11. D'hooge J, Heimdal A, Jamal F, Kukulski T, Bijnens B, Rademakers F, Hatle L, Suetens P, Sutherland GR. Regional strain and strain rate measurements by cardiac ultrasound: principles, implementation and limitations. *Eur J Echocardiogr* 1: 154–170, 2000. doi:10.1053/euje.2000.0031.
12. DiNino E, Gartman EJ, Sethi JM, McCool FD. Diaphragm ultrasound as a predictor of successful extubation from mechanical ventilation. *Thorax* 69: 423–427, 2014. doi:10.1136/thoraxjnl-2013-204111.
13. Doorduyn J, Sinderby CA, Beck J, Stegeman DF, van Hees HW, van der Hoeven JG, Heunks LM. The calcium sensitizer levosimendan improves human diaphragm function. *Am J Respir Crit Care Med* 185: 90–95, 2012. doi:10.1164/rccm.201107-1268OC.
14. Doorduyn J, Sinderby CA, Beck J, van der Hoeven JG, Heunks LM. Assisted ventilation in patients with acute respiratory distress syndrome: lung-distending pressure and patient-ventilator interaction. *Anesthesiology* 123: 181–190, 2015. doi:10.1097/ALN.0000000000000694.
15. Doorduyn J, van Hees HW, van der Hoeven JG, Heunks LM. Monitoring of the respiratory muscles in the critically ill. *Am J Respir Crit Care Med* 187: 20–27, 2013. doi:10.1164/rccm.201206-1117CP.
16. Ebihara S, Hussain SN, Danialou G, Cho WK, Gottfried SB, Petrof BJ. Mechanical ventilation protects against diaphragm injury in sepsis: interaction of oxidative and mechanical stresses. *Am J Respir Crit Care Med* 165: 221–228, 2002. doi:10.1164/ajrccm.165.2.2108041.
17. Gandevia SC, McKenzie DK, Plassman BL. Activation of human respiratory muscles during different voluntary manoeuvres. *J Physiol* 428: 387–403, 1990. doi:10.1113/jphysiol.1990.sp018218.
18. Goligher EC, Fan E, Herridge MS, Murray A, Vorona S, Brace D, Rittayamai N, Lanys A, Tomlinson G, Singh JM, Bolz SS, Rubenfeld GD, Kavanagh BP, Brochard LJ, Ferguson ND. Evolution of diaphragm thickness during mechanical ventilation. impact of inspiratory effort. *Am J Respir Crit Care Med* 192: 1080–1088, 2015. doi:10.1164/rccm.201503-0620OC.
19. Goligher EC, Laghi F, Detsky ME, Farias P, Murray A, Brace D, Brochard LJ, Bolz SS, Rubenfeld GD, Kavanagh BP, Ferguson ND. Measuring diaphragm thickness with ultrasound in mechanically ventilated patients: feasibility, reproducibility and validity. *Intensive Care Med* 41: 642–649, 2015. [Erratum. *Intensive Care Med* 41: 734, 2015.] doi:10.1007/s00134-015-3724-2.
20. Hatam N, Goetzenich A, Rossaint R, Karfis I, Bickenbach J, Autschbach R, Marx G, Bruells CS. A novel application for assessing diaphragmatic function by ultrasonic deformation analysis in noninvasively ventilated healthy young adults. *Ultraschall Med* 35: 540–546, 2014. doi:10.1055/s-0034-1366090.
21. Hermans G, Agten A, Testelmans D, Decramer M, Gayan-Ramirez G. Increased duration of mechanical ventilation is associated with decreased diaphragmatic force: a prospective observational study. *Crit Care* 14: R127, 2010. doi:10.1186/cc9094.
22. Heunks LM, Doorduyn J, van der Hoeven JG. Monitoring and preventing diaphragm injury. *Curr Opin Crit Care* 21: 34–41, 2015. doi:10.1097/MCC.0000000000000168.
23. Hooijman PE, Beishuizen A, Witt CC, de Waard MC, Girbes AR, Spoelstra-de Man AM, Niessen HW, Manders E, van Hees HW, van den Brom CE, Silderhuis V, Lawlor MW, Labeit S, Stienen GJ, Hartemink KJ, Paul MA, Heunks LM, Ottenheim CA. Diaphragm muscle fiber weakness and ubiquitin-proteasome activation in critically ill patients. *Am J Respir Crit Care Med* 191: 1126–1138, 2015. doi:10.1164/rccm.201412-2214OC.
24. Jaber S, Petrof BJ, Jung B, Chanques G, Berthet JP, Rabuel C, Bouyabrine H, Courouble P, Koechlin-Ramonatxo C, Sebbane M, Similowski T, Scheuermann V, Mebazaa A, Capdevila X, Mornet D, Mercier J, Lacampagne A, Philips A, Matecki S. Rapidly progressive diaphragmatic weakness and injury during mechanical ventilation in humans. *Am J Respir Crit Care Med* 183: 364–371, 2011. doi:10.1164/rccm.201004-0670OC.
25. Kim WY, Suh HJ, Hong SB, Koh Y, Lim CM. Diaphragm dysfunction assessed by ultrasonography: influence on weaning from mechanical ventilation. *Crit Care Med* 39: 2627–2630, 2011. doi:10.1097/CCM.0b013e3182266408.
26. Kunose K, Agarwal S, Marwick TH, Griffin BP, Popović ZB. Decision making in asymptomatic aortic regurgitation in the era of guidelines: incremental values of resting and exercise cardiac dysfunction. *Circ Cardiovasc Imaging* 7: 352–362, 2014. doi:10.1161/CIRCIMAGING.113.001177.
28. Laghi F, Cattapan SE, Jubran A, Parthasarathy S, Warshawsky P, Choi YS, Tobin MJ. Is weaning failure caused by low-frequency fatigue of the diaphragm? *Am J Respir Crit Care Med* 167: 120–127, 2003. doi:10.1164/rccm.200210-1246OC.
29. Lerolle N, Guérot E, Dimassi S, Zegdi R, Faisy C, Fagon JY, Diehl JL. Ultrasonographic diagnostic criterion for severe diaphragmatic dysfunction after cardiac surgery. *Chest* 135: 401–407, 2009. doi:10.1378/chest.08-1531.
30. Levine S, Nguyen T, Taylor N, Friscia ME, Budak MT, Rothenberg P, Zhu J, Sachdeva R, Sonnad S, Kaiser LR, Rubinstein NA, Powers SK, Shrager JB. Rapid disuse atrophy of diaphragm fibers in mechanically ventilated humans. *N Engl J Med* 358: 1327–1335, 2008. doi:10.1056/NEJMoa070447.
31. Matamis D, Soilemezi E, Tsagourias M, Akoumianaki E, Dimassi S, Boroli F, Richard JC, Brochard L. Sonographic evaluation of the diaphragm in critically ill patients. Technique and clinical applications. *Intensive Care Med* 39: 801–810, 2013. doi:10.1007/s00134-013-2823-1.
32. McKenzie DK, Butler JE, Gandevia SC. Respiratory muscle function and activation in chronic obstructive pulmonary disease. *J Appl Physiol* (1985) 107: 621–629, 2009. doi:10.1152/jappphysiol.00163.2009.
33. Oppersma E, Hatam N, Doorduyn J, van der Hoeven JG, Marx G, Goetzenich A, Heunks LM, Bruells CS. Speckle tracking echography allows sonographic assessment of diaphragmatic loading (Abstract). *Eur Respir J* 48: PA3564, 2016.
34. Orde SR, Boon AJ, Firth DG, Villarraga HR, Sekiguchi H. Diaphragm assessment by two dimensional speckle tracking imaging in normal subjects. *BMC Anesthesiol* 16: 43, 2016. doi:10.1186/s12871-016-0201-6.
35. Orozco-Levi M, Lloreta J, Minguela J, Serrano S, Broquetas JM, Gea J. Injury of the human diaphragm associated with exertion and chronic obstructive pulmonary disease. *Am J Respir Crit Care Med* 164: 1734–1739, 2001. doi:10.1164/ajrccm.164.9.2011150.
36. Parthasarathy S, Jubran A, Laghi F, Tobin MJ. Sternomastoid, rib cage, and expiratory muscle activity during weaning failure. *J Appl Physiol* (1985) 103: 140–147, 2007. doi:10.1152/jappphysiol.00904.2006.
37. Reid WD, Belcastro AN. Time course of diaphragm injury and calpain activity during resistive loading. *Am J Respir Crit Care Med* 162: 1801–1806, 2000. doi:10.1164/ajrccm.162.5.9906033.
38. Smiseth OA, Torp H, Opdahl A, Haugaa KH, Urheim S. Myocardial strain imaging: how useful is it in clinical decision making? *Eur Heart J* 37: 1196–1207, 2016. doi:10.1093/eurheartj/ehv529.
39. Ueki J, De Bruin PF, Pride NB. In vivo assessment of diaphragm contraction by ultrasound in normal subjects. *Thorax* 50: 1157–1161, 1995. doi:10.1136/thx.50.11.1157.
40. Umbrello M, Formenti P, Longhi D, Galimberti A, Piva I, Pezzi A, Mistraretti G, Marini JJ, Iapichino G. Diaphragm ultrasound as indicator of respiratory effort in critically ill patients undergoing assisted mechanical ventilation: a pilot clinical study. *Crit Care* 19: 161, 2015. doi:10.1186/s13054-015-0894-9.
41. Urheim S, Edvardsen T, Torp H, Angelsen B, Smiseth OA. Myocardial strain by Doppler echocardiography. Validation of a new method to quantify regional myocardial function. *Circulation* 102: 1158–1164, 2000. doi:10.1161/01.CIR.102.10.1158.
42. Vivier E, Mekontso Dessap A, Dimassi S, Vargas F, Lyazidi A, Thille AW, Brochard L. Diaphragm ultrasonography to estimate the work of

- breathing during non-invasive ventilation. *Intensive Care Med* 38: 796–803, 2012. doi:[10.1007/s00134-012-2547-7](https://doi.org/10.1007/s00134-012-2547-7).
43. **Waldman LK, Fung YC, Covell JW.** Transmural myocardial deformation in the canine left ventricle. Normal in vivo three-dimensional finite strains. *Circ Res* 57: 152–163, 1985. doi:[10.1161/01.RES.57.1.152](https://doi.org/10.1161/01.RES.57.1.152).
44. **Yingchoncharoen T, Gibby C, Rodriguez LL, Grimm RA, Marwick TH.** Association of myocardial deformation with outcome in asymptomatic aortic stenosis with normal ejection fraction. *Circ Cardiovasc Imaging* 5: 719–725, 2012. doi:[10.1161/CIRCIMAGING.112.977348](https://doi.org/10.1161/CIRCIMAGING.112.977348).

